

Planar Juggling of a Devil-Stick using Discrete VHCs

Aakash Khandelwal, and Ranjan Mukherjee, *Senior Member*

Abstract—Planar juggling of a devil-stick using impulsive inputs is addressed using the concept of discrete virtual holonomic constraints (DVHC). The location of the center-of-mass of the devil-stick is specified in terms of its orientation at the discrete instants when impulsive control inputs are applied. The discrete zero dynamics (DZD) resulting from the choice of DVHC provides conditions for stable juggling. A control design that enforces the DVHC and an orbit stabilizing controller are presented. The approach is validated in simulation.

Index Terms—Devil-stick, impulse controlled Poincaré map, nonprehensile manipulation, orbital stabilization, virtual holonomic constraints.

NOMENCLATURE

g	acceleration due to gravity, (m/s ²)
h_x, h_y	Cartesian coordinates of center-of-mass of the devil-stick, (m)
ℓ	length of the devil-stick, (m)
m	mass of the devil-stick, (kg)
r	distance of point of application of impulsive force from center-of-mass of the devil-stick, (m)
v_x, v_y	Cartesian components of velocity of center-of-mass of the devil-stick, (m/s)
I	impulse of impulsive force applied on the devil-stick, (Ns)
J	mass moment of inertia of the devil-stick about its center-of-mass, (kgm ²)
θ	orientation of the devil-stick, measured positive counter-clockwise with respect to the horizontal axis, (rad)
ω	angular velocity of the devil-stick, (rad/s)

I. INTRODUCTION

We consider the problem of planar juggling of a devil-stick, which represents a nonprehensile manipulation task using intermittent impulsive inputs. The dynamics and control of juggling point objects, described by position alone, has been considered in [1]–[6], with many works modeling the combined object-robot system with associated unilateral constraints and impact laws. In contrast to point objects, juggling a devil-stick [7]–[10] requires modeling orientation in addition to position.

The dynamics and closed-loop control design for planar *symmetric* juggling appeared in [8], [9]. A coordinate transformation was used to transform the orbital stabilization problem to one of fixed-point stabilization using a Poincaré

map in a rotating reference frame. Consequently, the dynamic model only permitted orbits with states that are *symmetric* about the vertical axis.

In this paper, we use the notion of discrete virtual holonomic constraints (DVHCs), introduced in [11], to define the trajectory of the devil-stick at discrete instants directly in the inertial frame. Similar to VHCs [12]–[15], DVHCs are geometric constraints on the generalized coordinates that avoid the need for tracking a time-varying reference trajectory. However, while VHCs are enforced using continuous feedback such that they are satisfied for all time, DVHCs are enforced using discrete feedback and are satisfied only at the instants when impulsive inputs are applied. The work in this paper extends the concept of DVHCs from *rotations* to *oscillations* of the passive coordinate for the dynamical system in [11]. Just like the zero dynamics induced by VHCs, the discrete zero dynamics (DZD) induced by DVHCs can be used to infer system stability. The DZD derived in this paper demonstrates that the dynamics of planar devil-stick juggling is far richer than that presented in [8].

The main contributions of this work are highlighted below, particularly in comparison to [8]:

- The dynamics and trajectory design are performed in the inertial reference frame, eliminating the need for coordinate transformation prior to every control action.
- It is not assumed *a priori* that the devil-stick is juggled between configurations that are symmetric in both position and velocity about the vertical axis.
- The system permits infinitely many 2-periodic orbits, *i.e.*, juggling motions, which are not necessarily symmetric about the vertical axis.
- The symmetric juggling motion in [8] is shown to be a special case of the family of orbits generated by the DVHCs chosen in this paper.

The impulse controlled Poincaré map (ICPM) approach [16], which was used to stabilize the fixed point associated with planar symmetric juggling in the rotating reference frame in [9] is adapted to stabilize any 2-periodic juggling motion.

This paper is organized as follows. In Section II, we define the planar juggling problem and present the hybrid dynamics of the system. In Section III, we present our choice of DVHCs and a control design that enforces them. In Section IV, we derive the DZD, which provides conditions for stable, periodic juggling. In Section V, we describe a method to stabilize a desired juggling motion. In Section VI, we validate the approach using simulations.

This work was supported by the National Science Foundation, under Grant CMMI-2043464

The authors are with the Department of Mechanical Engineering, Michigan State University, East Lansing, MI 48824, USA
khandel10@egr.msu.edu, mukherji@egr.msu.edu

II. SYSTEM DYNAMICS

A. System Description

Consider the three-DOF devil-stick in the vertical xy plane in Fig.1. Its configuration is described by the independent generalized coordinates (h_x, h_y, θ) . It is juggled using the control inputs I and r , where I is the impulse applied normal to the devil-stick and r is the distance of its point of application from the center-of-mass. The devil-stick is juggled between the orientations $\theta^{\text{odd}} \in (0, \pi/2)$ and $\theta^{\text{even}} \in (\pi/2, \pi)$, which are chosen *a priori*. Therefore, $\theta \in [\theta^{\text{odd}}, \theta^{\text{even}}] \forall t$ during the juggling task. Impulsive inputs are applied alternately at $\theta = \theta^{\text{odd}}$ and $\theta = \theta^{\text{even}}$, and the devil-stick falls freely under gravity between successive applications of impulsive inputs, making the resulting system dynamics hybrid. Since there is one fewer control input than the number of generalized coordinates, the system is under-actuated with one passive DOF. The vector of generalized coordinates is

$$q \triangleq [h^T \mid \theta]^T, \quad h = [h_x \ h_y]^T \quad (1)$$

where $h \in \mathbb{R}^2$ are the active coordinates and $\theta \in S^1$ is the passive coordinate. The vector of generalized velocities is

$$\dot{q} \triangleq [v^T \mid \omega]^T, \quad v = [v_x \ v_y]^T \quad (2)$$

where $v \in \mathbb{R}^2$ and $\omega \in \mathbb{R}$.

B. Hybrid Dynamic Model

The hybrid dynamic model captures a single impulsive actuation¹, followed by a flight phase under gravity. Using k to represent instants immediately prior to applications of impulsive inputs, the dynamics of the active positions and velocities are [11]

$$h(k+1) = h(k) + v(k)\delta_k + \begin{bmatrix} -\sin \theta_k \\ \cos \theta_k \end{bmatrix} \frac{I_k \delta_k}{m} + \begin{bmatrix} 0 \\ -\frac{1}{2}g\delta_k^2 \end{bmatrix} \quad (3)$$

$$v(k+1) = v(k) + \begin{bmatrix} -\sin \theta_k \\ \cos \theta_k \end{bmatrix} \frac{I_k}{m} + \begin{bmatrix} 0 \\ -g\delta_k \end{bmatrix} \quad (4)$$

where δ_k is the time-of-flight, *i.e.*, the interval between application of the k -th and $(k+1)$ -th impulsive inputs. Without

¹Impulsive inputs cause no change in position coordinates and finite jumps in velocities [16].

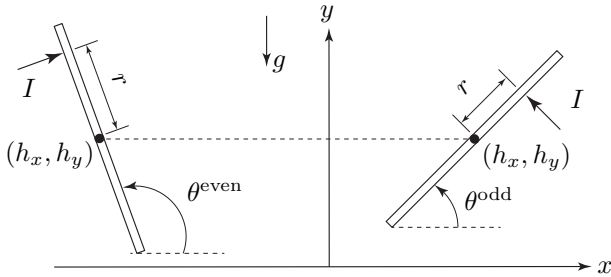


Fig. 1. A devil-stick in the vertical plane with configuration variables (h_x, h_y, θ) , and control variables (I, r) .

loss of generality, we assert that the angular configurations θ_k at which impulsive inputs are applied are such that

$$\theta_k = \begin{cases} \theta^{\text{odd}}, & k \text{ odd} \\ \theta^{\text{even}}, & k \text{ even} \end{cases} \quad (5)$$

The change in orientation between successive applications of the impulsive input is described by

$$\theta_{k+1} - \theta_k = (-1)^{k+1} \Delta\theta^*, \quad \Delta\theta^* \triangleq \theta^{\text{even}} - \theta^{\text{odd}} \quad (6)$$

where $\Delta\theta^* > 0$. It immediately follows from (5) or (6) that θ is periodic with period-2, *i.e.*,

$$\theta_{k+2} = \theta_k \quad (7)$$

The hybrid dynamics of the passive coordinate and velocity are given by [11]

$$\theta_{k+1} = \theta_k + \omega_k \delta_k + \frac{I_k r_k}{J} \delta_k \quad (8)$$

$$\omega_{k+1} = \omega_k + \frac{I_k r_k}{J} \quad (9)$$

It follows from (6), (8), and (9) that the time-of-flight is

$$\delta_k = \frac{(-1)^{k+1} \Delta\theta^*}{\omega_k + \frac{I_k r_k}{J}} \Rightarrow \delta_k = \frac{(-1)^{k+1} \Delta\theta^*}{\omega_{k+1}} \quad (10)$$

For feasible planar juggling, $\omega_k < 0$ when k is odd ($\theta_k = \theta^{\text{odd}}$) and $\omega_k > 0$ when k is even ($\theta_k = \theta^{\text{even}}$). It then follows from the above equation that $\delta_k > 0 \forall k$. Further, the control inputs $I_k > 0, r_k > 0$ produce a counterclockwise moment when k is odd, and $I_k < 0, r_k > 0$ produce a clockwise moment when k is even - see Fig.1.

III. DISCRETE VIRTUAL HOLONOMIC CONSTRAINTS

A. Constraints on Positions

We use discrete virtual holonomic constraints (DVHCs) [11] to define the trajectory of the center-of-mass of the devil-stick in terms of its orientation at the instants k that impulsive inputs are applied on the devil-stick:

$$\rho_k \triangleq h(k) - \Phi(\theta_k) = 0, \quad \Phi : S^1 \rightarrow \mathbb{R}^2, \quad k = 1, 2, \dots \quad (11)$$

where $\Phi : S^1 \rightarrow \mathbb{R}^2$ is given by

$$\Phi(\theta_k) = \begin{bmatrix} \alpha \tan \theta_k \\ \beta \end{bmatrix} \quad (12)$$

where $\alpha, \beta \in \mathbb{R}^+$ are parameters that can be chosen arbitrarily. It follows from (5) that the above DVHC places the center-of-mass of the devil-stick at $h(k) = [\alpha \tan \theta^{\text{odd}} \ \beta]^T$ when k is odd, and $h(k) = [\alpha \tan \theta^{\text{even}} \ \beta]^T$ when k is even. From the choices of θ^{odd} and θ^{even} in Section II-A, it follows that $h_x(k) > 0$ when k is odd, and $h_x(k) < 0$ when k is even. In particular, if $\theta^{\text{even}} = \pi - \theta^{\text{odd}}$, *i.e.*, impulsive inputs are applied when the orientation of the devil-stick is symmetric about the vertical y axis, $h_x(k+1) = -h_x(k) \forall k$. The value of $h_y(k)$ is constant $\forall k$.

Remark 1: The results for planar symmetric juggling in [8] are a special case for the DVHC in (12) - see Section

IV-C. Using different DVHCs, different juggling motions may be obtained; *e.g.*, the value of $h_y(k)$ can be varied with k by replacing β in (12) by some function of θ_k .

B. Constraints on Velocities

We begin by rewriting (3) as

$$h(k+1) - h(k) = \left\{ v(k) + \begin{bmatrix} -\sin \theta_k \\ \cos \theta_k \end{bmatrix} \frac{I_k}{m} + \begin{bmatrix} 0 \\ -g\delta_k \end{bmatrix} \right\} \delta_k + \begin{bmatrix} 0 \\ \frac{1}{2}g\delta_k^2 \end{bmatrix} \quad (13)$$

Using (4) in the above equation, we obtain

$$h(k+1) - h(k) = v(k+1)\delta_k + \begin{bmatrix} 0 \\ \frac{1}{2}g\delta_k^2 \end{bmatrix} \quad (14)$$

Using the DVHC from (11) at k and $k+1$ in the above equation, we obtain

$$\Phi(\theta_{k+1}) - \Phi(\theta_k) = v(k+1)\delta_k + \begin{bmatrix} 0 \\ \frac{1}{2}g\delta_k^2 \end{bmatrix} \quad (15)$$

The above equation can be rewritten as

$$v(k+1) = \frac{1}{\delta_k} [\Phi(\theta_{k+1}) - \Phi(\theta_k)] - \begin{bmatrix} 0 \\ \frac{1}{2}g\delta_k \end{bmatrix} \quad (16)$$

Replacing the instances of $k+1$ by k in the above equation, we obtain

$$v(k) = \frac{1}{\delta_{k-1}} [\Phi(\theta_k) - \Phi(\theta_{k-1})] - \begin{bmatrix} 0 \\ \frac{1}{2}g\delta_{k-1} \end{bmatrix} \quad (17)$$

From (7) it follows that $\theta_{k-1} = \theta_{k+1}$, and from (10) it follows that $\delta_{k-1} = (-1)^k \Delta\theta^* / \omega_k$. Thus, (17) can be rewritten as

$$v(k) = \frac{(-1)^k \omega_k}{\Delta\theta^*} [\Phi(\theta_k) - \Phi(\theta_{k+1})] - \begin{bmatrix} 0 \\ \frac{(-1)^k g \Delta\theta^*}{2\omega_k} \end{bmatrix} \quad (18)$$

The constraint on velocities is therefore given by

$$D\rho_k \triangleq v(k) - \Psi(\theta_k, \omega_k) = 0, \quad k = 1, 2, \dots \quad (19)$$

where Ψ is given by

$$\Psi(\theta_k, \omega_k) = \frac{(-1)^k \omega_k}{\Delta\theta^*} [\Phi(\theta_k) - \Phi(\theta_{k+1})] - \begin{bmatrix} 0 \\ \frac{(-1)^k g \Delta\theta^*}{2\omega_k} \end{bmatrix} \quad (20)$$

Remark 2: The value of θ_{k+1} is known at k from (6). In the above equation and subsequent equations, we use θ_{k+1} for brevity, in place of the full expression $\theta_k + (-1)^{k+1} \Delta\theta^*$ involving θ_k alone; $\Psi(\theta_k, \omega_k)$ remains a function of only the passive coordinate and passive velocity at k .

Using (12) in the above equation and simplifying,

$$\Psi(\theta_k, \omega_k) = \frac{(-1)^k \omega_k}{\Delta\theta^*} \begin{bmatrix} \alpha(\tan \theta_k - \tan \theta_{k+1}) \\ 0 \end{bmatrix} - \begin{bmatrix} 0 \\ \frac{(-1)^k g \Delta\theta^*}{2\omega_k} \end{bmatrix} \quad (21)$$

C. Control Design Enforcing the DVHC

We seek the control inputs that enforce the DVHC. We first treat δ_k as an input for simplicity. Using (11) and (19) in (3), we obtain

$$\rho_{k+1} + \Phi(\theta_{k+1}) = [\rho_k + \Phi(\theta_k)] + [D\rho_k + \Psi(\theta_k, \omega_k)]\delta_k + \begin{bmatrix} -\sin \theta_k \\ \cos \theta_k \end{bmatrix} \frac{I_k \delta_k}{m} + \begin{bmatrix} 0 \\ -\frac{1}{2}g\delta_k^2 \end{bmatrix} \quad (22)$$

Exponential convergence to $\rho_k = 0$ is achieved if

$$\rho_{k+1} = \lambda \rho_k, \quad \lambda \triangleq \text{diag} [\lambda_x \quad \lambda_y], \quad \lambda_x, \lambda_y \in [0, 1) \quad (23)$$

We define $\eta_k \triangleq \Phi(\theta_{k+1}) - \Phi(\theta_k)$ to rewrite (22) as

$$(\lambda - 1)\rho_k + \eta_k = [D\rho_k + \Psi(\theta_k, \omega_k)]\delta_k + \begin{bmatrix} -\sin \theta_k \\ \cos \theta_k \end{bmatrix} \frac{I_k \delta_k}{m} + \begin{bmatrix} 0 \\ -\frac{1}{2}g\delta_k^2 \end{bmatrix} \quad (24)$$

whose x and y components can be expressed separately as

$$(\lambda_x - 1)\rho_{xk} + \eta_{xk} = [D\rho_{xk} + \Psi_x(\theta_k, \omega_k)]\delta_k - \frac{I_k \delta_k}{m} \sin \theta_k \quad (25a)$$

$$(\lambda_y - 1)\rho_{yk} + \eta_{yk} = [D\rho_{yk} + \Psi_y(\theta_k, \omega_k)]\delta_k + \frac{1}{2}g\delta_k^2 = \frac{I_k \delta_k}{m} \cos \theta_k \quad (25b)$$

where $\rho_k = [\rho_{xk} \quad \rho_{yk}]^T$, $D\rho_k = [D\rho_{xk} \quad D\rho_{yk}]^T$, $\eta_k = [\eta_{xk} \quad \eta_{yk}]^T$ and $\Psi = [\Psi_x \quad \Psi_y]^T$. Since $\sin \theta_k \neq 0$ for any θ_k in (5), we eliminate I_k between (25a) and (25b) to obtain

$$\frac{1}{2}g\delta_k^2 - \{[D\rho_{xk} + \Psi_x(\theta_k, \omega_k)] \cot \theta_k + [D\rho_{yk} + \Psi_y(\theta_k, \omega_k)]\} \delta_k + [\eta_{xk} \cot \theta_k + \eta_{yk}] = 0 + (\lambda_x - 1)\rho_{xk} \cot \theta_k + (\lambda_y - 1)\rho_{yk} = 0 \quad (26)$$

The time-of-flight δ_k is obtained by solving the above equation. The value of I_k is then obtained from (25a) as

$$I_k = -\frac{m \{(\lambda_x - 1)\rho_{xk} + \eta_{xk} - [D\rho_{xk} + \Psi_x(\theta_k, \omega_k)]\delta_k\}}{\delta_k \sin \theta_k} \quad (27)$$

Finally, the value of r_k is obtained from (10) as

$$r_k = \frac{(-1)^{k+1} J \Delta\theta^*}{I_k \delta_k} - \frac{J \omega_k}{I_k} \quad (28)$$

Remark 3: The control design must ensure that the time-of-flight $\delta_k > 0$, and the point of application of the impulse lies on the devil-stick, *i.e.*, $r_k \in (-\ell/2, \ell/2)$.

Remark 4: It can be shown that [11]

$$D\rho_{k+1} = \frac{(\lambda - 1)\rho_k}{\delta_k} \quad (29)$$

which ensures that $D\rho_k \rightarrow 0$ as $\rho_k \rightarrow 0$, and the control design presented in this section enforces the DVHC.

If $\rho_k = 0$ and $D\rho_k = 0$, explicit solutions of the time-of-flight and control inputs are obtained upon simplification of (26), (27) and (28) as

$$\delta_k = \frac{(-1)^k 2\omega_k \alpha}{g\Delta\theta^*} \left(1 - \frac{\tan \theta_{k+1}}{\tan \theta_k} \right) \quad (30)$$

$$I_k = \frac{(-1)^k m}{\cos \theta_k} \left[\frac{\omega_k \alpha}{\Delta\theta^*} \left(1 - \frac{\tan \theta_{k+1}}{\tan \theta_k} \right) + \frac{g\Delta\theta^*}{2\omega_k} \right] \quad (31)$$

$$r_k = \frac{(-1)^{k+1} J\Delta\theta^* \cos \theta_k}{m\alpha \left(1 - \frac{\tan \theta_{k+1}}{\tan \theta_k} \right)} \quad (32)$$

IV. DISCRETE ZERO DYNAMICS

A. Derivation

The discrete zero dynamics (DZD) provides the dynamics of passive coordinate θ and passive velocity ω when the DVHCs are satisfied, and system trajectories evolve such that $\rho_k \equiv 0 \Rightarrow h(k) \equiv \Phi(\theta_k)$ and $D\rho_k \equiv 0 \Rightarrow v(k) \equiv \Psi(\theta_k, \omega_k)$. It follows from (19) and (21) that

$$v_x(k) = \frac{(-1)^k \omega_k \alpha}{\Delta\theta^*} (\tan \theta_k - \tan \theta_{k+1}) \quad (33a)$$

$$v_y(k) = -\frac{(-1)^k g\Delta\theta^*}{2\omega_k} \quad (33b)$$

Similarly, it follows from (7), (19) and (21) that

$$v_x(k+1) = \frac{(-1)^k \omega_{k+1} \alpha}{\Delta\theta^*} (\tan \theta_k - \tan \theta_{k+1}) \quad (34a)$$

$$v_y(k+1) = \frac{(-1)^k g\Delta\theta^*}{2\omega_{k+1}} \quad (34b)$$

The input I_k can be eliminated between the two equations in (4) to obtain

$$\begin{aligned} & v_x(k+1) \cos \theta_k + v_y(k+1) \sin \theta_k \\ &= v_x(k) \cos \theta_k + v_y(k) \sin \theta_k - g\delta_k \sin \theta_k \end{aligned} \quad (35)$$

Using (10), the above equation may be rewritten as

$$\begin{aligned} & v_x(k+1) \cos \theta_k + v_y(k+1) \sin \theta_k \\ &= v_x(k) \cos \theta_k + v_y(k) \sin \theta_k + \frac{(-1)^k g\Delta\theta^*}{\omega_{k+1}} \sin \theta_k \end{aligned} \quad (36)$$

Using (33) and (34) in (36) and simplifying, we obtain

$$\frac{g\Delta\theta^{*2}}{2\omega_k \omega_{k+1}} + \alpha \left(1 - \frac{\tan \theta_{k+1}}{\tan \theta_k} \right) = 0 \quad (37)$$

Equations (6) and (37) together define the DZD:

$$\begin{aligned} & \mathcal{Z}(\theta_k, \omega_k, \theta_{k+1}, \omega_{k+1}) = 0 \\ & \mathcal{Z} \triangleq \left[\frac{\theta_{k+1} - \theta_k - (-1)^{k+1} \Delta\theta^*}{\frac{g\Delta\theta^{*2}}{2\omega_k \omega_{k+1}} + \alpha \left(1 - \frac{\tan \theta_{k+1}}{\tan \theta_k} \right)} \right] \end{aligned} \quad (38)$$

and describe the system behavior when the DVHC in (11) is identically satisfied. The nature of solutions to (38) governs the stability and periodicity of juggling. Conditions for stable, periodic juggling are presented next.

B. Stable Juggling

Theorem 1: The dynamical system in (38) is periodic with period-2, i.e., $\theta_{k+2} = \theta_k$ and $\omega_{k+2} = \omega_k$, if and only if

$$\theta^{\text{even}} = \pi - \theta^{\text{odd}} \quad (39)$$

i.e., the orientations at which impulsive inputs are applied on the devil-stick are symmetric about the vertical axis.

Proof: The 2-periodicity of θ follows directly from (7). To establish 2-periodicity of ω , observe that (37) can be rewritten

$$\frac{g\Delta\theta^{*2}}{2\omega_k \omega_{k+1}} = \alpha \left(\frac{\tan \theta_{k+1}}{\tan \theta_k} - 1 \right) \quad (40)$$

It follows that

$$\frac{g\Delta\theta^{*2}}{2\omega_{k+1} \omega_{k+2}} = \alpha \left(\frac{\tan \theta_k}{\tan \theta_{k+1}} - 1 \right) \quad (41)$$

where (7) has been used to replace θ_{k+2} by θ_k . Dividing (40) by (41) and simplifying, we obtain

$$\omega_{k+2} = -\frac{\tan \theta_{k+1}}{\tan \theta_k} \omega_k \quad (42)$$

It follows that

$$\omega_{k+2} = \omega_k \iff \tan \theta_{k+1} = -\tan \theta_k \quad \forall k$$

To show sufficiency, observe that (5) and (39) imply

$$\theta_{k+1} = \pi - \theta_k \quad \forall k \implies \tan \theta_{k+1} = -\tan \theta_k \quad \forall k$$

To show necessity, observe that $\tan \theta_{k+1} = -\tan \theta_k$ can be solved as

$$\theta_{k+1} = n\pi - \arctan(\tan \theta_k), \quad n \in \mathbb{Z}$$

If $\theta_k = \theta^{\text{odd}}$, $\arctan(\tan \theta_k) = \theta^{\text{odd}}$ since $\theta^{\text{odd}} \in (0, \pi/2)$. It follows from (5) that $\theta_{k+1} = \theta^{\text{even}}$, and $n = 1$ provides the only feasible solution $\theta^{\text{even}} = \pi - \theta^{\text{odd}}$ since $\theta^{\text{even}} \in (\pi/2, \pi)$. If $\theta_k = \theta^{\text{even}}$, $\arctan(\tan \theta_k) = \theta^{\text{even}} - \pi$ since $\theta^{\text{even}} \in (\pi/2, \pi)$. It follows from (5) that $\theta_{k+1} = \theta^{\text{odd}}$, and $n = 0$ provides the only feasible solution $\theta^{\text{odd}} = \pi - \theta^{\text{even}}$ since $\theta^{\text{odd}} \in (0, \pi/2)$, which implies $\theta^{\text{even}} = \pi - \theta^{\text{odd}}$. ■

Corollary 1: For the DVHC in (12), it is not possible to achieve stable juggling between orientations that are asymmetric about the vertical axis, i.e., $\theta^{\text{even}} \neq \pi - \theta^{\text{odd}}$.

Corollary 1 follows directly from (42). Theorem 1 implies that a unique stable, 2-periodic juggling motion corresponds to unique ω_k values for each $\theta_k \in \{\theta^{\text{odd}}, \theta^{\text{even}}\}$, where θ^{odd} and θ^{even} satisfy (39); these values are:

$$\omega_k = \begin{cases} \omega^*, & k \text{ odd} \\ -\frac{g\Delta\theta^{*2}}{4\omega^* \alpha}, & k \text{ even} \end{cases} \quad (43)$$

where $\omega^* < 0$ may be chosen arbitrarily, and the value of ω_k corresponding to even k is found from (37) with $(1 - \tan \theta_{k+1}/\tan \theta_k) = 2$, which follows from (39). Further, it follows from (30) and (43) that there exist the two unique times-of-flight

$$\delta_k = \begin{cases} -4\omega^* \alpha / (g\Delta\theta^*), & k \text{ odd} \\ -\Delta\theta^* / \omega^*, & k \text{ even} \end{cases} \quad (44)$$

From (31), (37), (39), and (43), we obtain

$$I_k = \frac{(-1)^k 2m\alpha}{\Delta\theta^* \cos \theta^{\text{odd}}} \left[\omega^* + \frac{g\Delta\theta^{*2}}{4\omega^*\alpha} \right] \quad (45)$$

which indicates that the *magnitude* of impulse applied at either symmetric orientation of the devil-stick is the same, with opposite signs. From (32) and (39), we obtain

$$r_k = \frac{J\Delta\theta^* \cos \theta^{\text{odd}}}{2m\alpha} \quad (46)$$

which implies that the location of application of the impulse is identical for either symmetric orientation of the devil-stick. These results demonstrate that the DZD (38) permits infinitely many stable, 2-periodic orbits when (39) holds, with each orbit corresponding to a unique choice of $\omega^* < 0$.

C. Planar Symmetric Juggling

A special juggling motion, which is symmetric in both orientation and angular velocity about the vertical [8], [9] occurs when (39) holds and

$$\omega^* = -\frac{\Delta\theta^*}{2} \sqrt{\frac{g}{\alpha}} \Rightarrow \omega_k = \begin{cases} \omega^*, & k \text{ odd} \\ -\omega^*, & k \text{ even} \end{cases} \quad (47)$$

for which $\delta_k = -\Delta\theta^*/\omega^* \forall k$. The steady-state solutions for states and control inputs in [8] are reproduced when ω^* is chosen as in (47) for the DVHC in (12).

V. STABILIZATION OF JUGGLING MOTION

A. Orbit Selection

A distinct stable juggling motion described by DVHCs (12) and velocity constraints (21), with θ^{odd} and θ^{even} chosen to satisfy (39), is the orbit²

$$\mathcal{O}^* = \{(q, \dot{q}) : h(k) = \Phi(\theta_k), v(k) = \Psi(\theta_k, \omega_k), \omega_k = \omega^* \forall \theta_k = \theta^{\text{odd}}\} \quad (48)$$

To stabilize \mathcal{O}^* , we define the section³

$$\Sigma = \{(q, \dot{q}) \in \mathbb{R}^2 \times S^1 \times \mathbb{R}^3 : \theta = \theta^{\text{odd}}, \omega < 0\} \quad (49)$$

on which the states are

$$z = [h^T \quad v^T \quad \omega]^T, \quad z \in \mathbb{R}^5 \quad (50)$$

For a system trajectory not on \mathcal{O}^* , we modify the inputs I and r only at $\theta_k = \theta^{\text{odd}}$ from the values in (27) and (28) such that the system trajectory is driven to \mathcal{O}^* . Since $\theta_{k+2} = \theta_k$, the hybrid dynamics of the system between successive intersections with Σ (involving two applications of the impulsive inputs) is given by

$$z(j+1) = \mathbb{P}[z(j), I(j), r(j)] \quad (51)$$

where $z(j)$ denotes the states on Σ immediately prior to application of inputs $I(j)$ and $r(j)$ on Σ . Note that for every intersection of the system trajectory with Σ , the increment in k is 2 while the increment in j is 1.

²The orbit can equivalently be specified based on $\omega_k \forall \theta_k = \theta^{\text{even}}$.

³The section can alternatively be chosen with $\theta = \theta^{\text{even}}, \omega > 0$.

B. Orbital Stabilization

If $(q, \dot{q}) \in \mathcal{O}^*$, the system trajectory lies on \mathcal{O}^* under the inputs from (27) and (28) alone. Therefore, the intersection of \mathcal{O}^* with Σ is a fixed point $z(j) = z^*, I(j) = I^*, r(j) = r^*$ of the map \mathbb{P} ; I^* and r^* are obtained from (45) and (46) respectively:

$$z^* = \mathbb{P}(z^*, I^*, r^*) \quad (52)$$

If $(q, \dot{q}) \notin \mathcal{O}^*$, the inputs (27) and (28) drive system trajectories to an orbit such that $\rho_k = 0$, but not necessarily the desired orbit \mathcal{O}^* . We stabilize \mathcal{O}^* by using the ICPM approach [16] to stabilize the fixed point z^* on Σ . First, linearize \mathbb{P} about $z(j) = z^*$ and $I(j) = I^*, r(j) = r^*$ as

$$e(j+1) = \mathcal{A}e(j) + \mathcal{B}u(j) \quad (53)$$

$$e(j) \triangleq z(j) - z^*, \quad u(j) \triangleq \begin{bmatrix} I(j) \\ r(j) \end{bmatrix} - \begin{bmatrix} I^* \\ r^* \end{bmatrix} \quad (54)$$

where $\mathcal{A} \in \mathbb{R}^{5 \times 5}$, $\mathcal{B} \in \mathbb{R}^{5 \times 2}$ may be computed numerically [11]. If the pair $(\mathcal{A}, \mathcal{B})$ is controllable, \mathcal{O}^* is asymptotically stabilized by the discrete feedback

$$u(j) = \mathcal{K}e(j) \quad (55)$$

where \mathcal{K} places the eigenvalues of $(\mathcal{A} + \mathcal{B}\mathcal{K})$ within the unit circle. Thus, for every intersection of the system trajectory with Σ , the applied inputs are

$$\begin{bmatrix} I(j) \\ r(j) \end{bmatrix} = \begin{bmatrix} I_k \\ r_k \end{bmatrix} + u(j) \quad (56)$$

where I_k and r_k are given by (27) and (28). The additional input $u(j)$ is not applied if the trajectory is sufficiently close to \mathcal{O}^* , i.e., $\|e(j)\|$ is sufficiently small.

VI. SIMULATION

The physical parameters of the devil-stick in SI units are:

$$m = 0.1, \quad \ell = 0.5, \quad J = \frac{1}{12}m\ell^2 = 0.0021$$

A. Enforcing the DVHC

We consider the DVHC in (12) with

$$\alpha = 0.6131, \quad \beta = 3 \quad (57)$$

The values of θ^{odd} and θ^{even} are chosen to be

$$\theta^{\text{odd}} = \pi/6, \quad \theta^{\text{even}} = \pi - \theta^{\text{odd}} = 5\pi/6 \quad (58)$$

which ensures that the DZD in (38) permits stable, 2-periodic orbits - see Theorem 1. The resulting value of $\Delta\theta^* = \pi/3$. The control inputs are obtained using (27) and (28) with

$$\lambda_x = \lambda_y = 0.5 \quad (59)$$

We consider the initial conditions

$$[q^T \quad \dot{q}^T]^T = [0.7 \quad 2.5 \quad 0.5236 \quad 0.9 \quad -2.0 \quad -5.7]^T \quad (60)$$

for which $\theta = \theta_1 = \theta^{\text{odd}}$ and $\rho_1 \neq 0$. The simulation results are shown in Fig.2 for $k = 1$ through $k = 20$, corresponding to a duration of approximately 9.80 s. The components of ρ_k are shown in Fig.2(a)-(b), and the components of $D\rho_k$ are

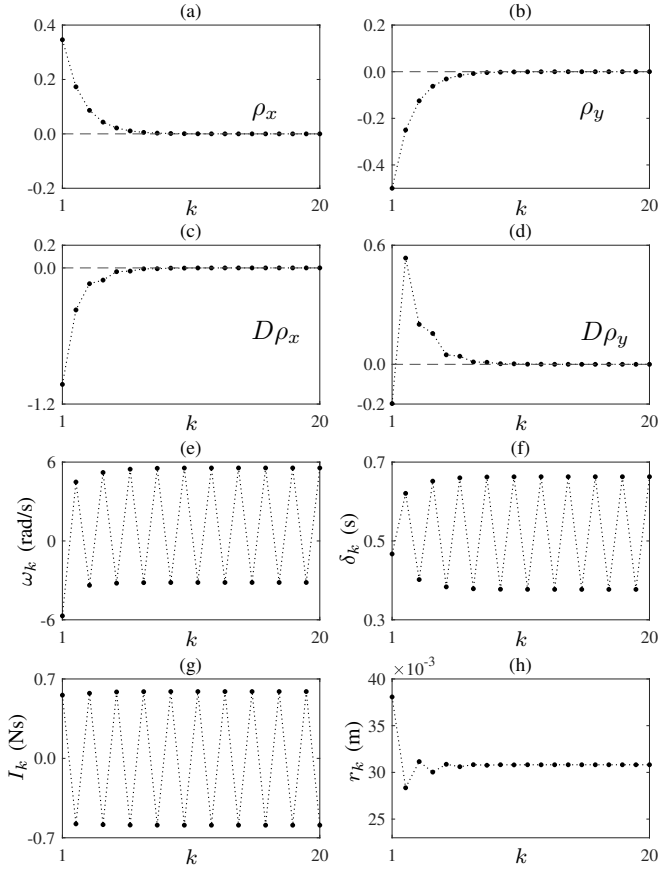


Fig. 2. Stabilization of 2-periodic juggling of a devil-stick from arbitrary initial conditions: (a)-(b) show the components of ρ_k , (c)-(d) show the components of $D\rho_k$, (e) shows the pre-impact angular velocity ω_k , (f) shows the time-of-flight δ_k , (g) shows the applied impulse I_k , and (h) shows the point of application r_k of the impulsive force.

shown in Fig.2(c)-(d). The plots demonstrate that the system trajectory converges to $\rho_k = 0$ exponentially. As the DVHC is enforced, the system settles to a stable, 2-periodic juggling motion with

$$\omega_k = \begin{cases} -3.1596, & k \text{ odd} \\ 5.5532, & k \text{ even} \end{cases}, \quad \delta_k = \begin{cases} 0.3771, & k \text{ odd} \\ 0.6629, & k \text{ even} \end{cases} \quad (61)$$

which agree with (43) and (44). The values of ω_k and δ_k are plotted in Fig.2(e) and Fig.2(f). The control inputs I_k and r_k are shown in Fig.2(g) and Fig.2(h) respectively. For the 2-periodic juggling motion in (61), $I_k = -(-1)^k \times 0.5890$ Ns and $r_k = 0.0308$ m, in accordance with (45) and (46). The trajectory of the center-of-mass of the devil-stick corresponding to these results is shown in Fig.3(a).

B. Stabilization of a Periodic Orbit

We now demonstrate the effectiveness of the controller described in Section V in stabilizing a desired orbit, specifically the orbit corresponding to planar symmetric juggling in [8], [9]. We consider the DVHC in (12) with the parameters in (57) and the same choices of θ^{odd} and θ^{even} in (58). Of the infinitely many stable, 2-periodic orbits, we choose to stabilize the orbit for which $\omega^* = -4.1888$, obtained from

(47). This results in $\delta_k = 0.5$ s $\forall k$ corresponding to stable juggling. This orbit can be described using (48) as

$$\mathcal{O}^* = \{(q, \dot{q}) : h(k) = \Phi(\theta_k), v(k) = \Psi(\theta_k, \omega_k), \omega_k = -4.1888 \forall \theta_k = \pi/3\} \quad (62)$$

We obtain the control inputs (27) and (28) with the same choice of λ as in (59). The section (49) on which the orbit stabilizing controller (56) acts is

$$\Sigma = \{(q, \dot{q}) \in \mathbb{R}^2 \times S^1 \times \mathbb{R}^3 : \theta = \pi/3, \omega < 0\} \quad (63)$$

The fixed point of the map \mathbb{P} in (52) corresponding to the orbit \mathcal{O}^* in (62) and the section Σ in (63) is

$$z^* = [0.3540 \quad 3.0000 \quad 1.4160 \quad -2.4525 \quad -4.1888]^T \\ I^* = 0.5664, \quad r^* = 0.0308 \quad (64)$$

The matrices \mathcal{A} and \mathcal{B} in (53) are

$$\mathcal{A} = \begin{bmatrix} 0.2500 & 0.0000 & 0.0000 & -0.0000 & -0.0000 \\ 0.0000 & 0.2500 & 0.0000 & 0.0000 & 0.0000 \\ -0.2500 & 0.4329 & 0.5001 & 0.2887 & 0.0000 \\ 0.4331 & 0.2495 & 0.8659 & 0.4999 & 0.0000 \\ -0.7398 & -1.2807 & -1.4794 & -0.8541 & -0.0000 \end{bmatrix} \\ \mathcal{B} = \begin{bmatrix} -0.0000 & 4.2847 & -12.2873 & -30.0787 & 36.3492 \\ 20.3351 & 31.1748 & -111.2006 & -200.6851 & 221.3658 \end{bmatrix}^T$$

While not all eigenvalues of \mathcal{A} lie within the unit circle, the pair $(\mathcal{A}, \mathcal{B})$ is controllable, and the gain matrix \mathcal{K} in (55) that asymptotically stabilizes \mathcal{O}^* is obtained using LQR with the weighting matrices $\mathcal{Q} = \mathbb{I}_5$, $\mathcal{R} = 2\mathbb{I}_2$ as

$$\mathcal{K} = \begin{bmatrix} 0.0961 & 0.0358 & 0.0398 & 0.0230 & 0.0000 \\ -0.0124 & -0.0017 & -0.0006 & -0.0003 & 0.0000 \end{bmatrix}$$

The same initial conditions (60) are used, and the simulation results are shown in Fig.4 for $k = 1$ through $k = 20$, a duration of approximately 9.59 s. The components of ρ_k are shown in Fig.4(a)-(b), and the components of $D\rho_k$ are shown in Fig.4(c)-(d). It is seen that the system trajectory converges to $\rho_k = 0$, and $D\rho_k \rightarrow 0$ as $\rho_k \rightarrow 0$. The values of ω_k , shown in Fig.4(e), converge to values in agreement with (47), $\omega^* = -4.1888$ rad/s, indicating stabilization of the orbit in (62). The time-of-flight, plotted in Fig.4(f), converges to the constant value $\delta_k = 0.5$ s. The control inputs I_k and r_k are

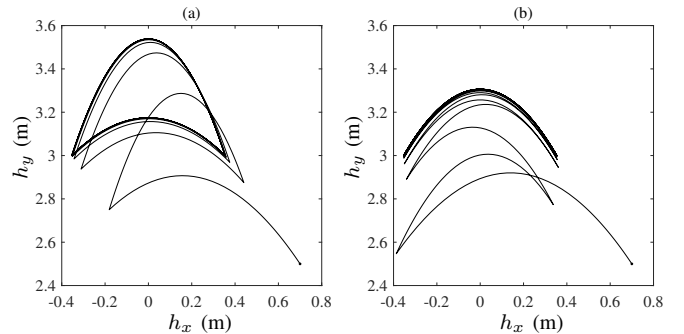


Fig. 3. Trajectory of the center-of-mass of the devil-stick corresponding to the results in (a) Fig. 2 showing 2-periodic juggling, and (b) Fig. 4 showing planar symmetric juggling.

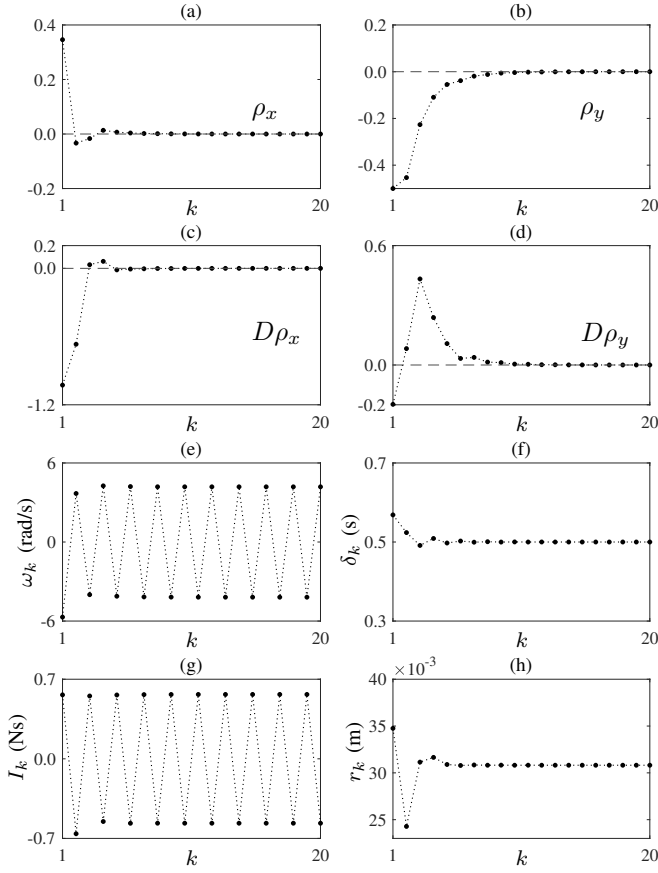


Fig. 4. Orbital stabilization of planar symmetric juggling of a devil-stick from arbitrary initial conditions: (a)-(b) show the components of ρ_k , (c)-(d) show the components of $D\rho_k$, (e) shows the pre-impact angular velocity ω_k , (f) shows the time-of-flight δ_k (g) shows the applied impulse I_k , and (h) shows the point of application r_k of the impulsive force.

shown in Fig.4(g) and Fig.4(h) respectively. The inputs are obtained from (56) for $j = 1, 2, \dots, 7$, i.e., $k = 1, 3, \dots, 13$. The controller $u(j)$ is inactive for $j > 7$ as the system trajectory is sufficiently close to \mathcal{O}^* . For planar symmetric juggling, $I_k = -(-1)^k \times 0.5664$ Ns and $r_k = 0.0308$ m in accordance with (45) and (46). The trajectory of the center-of-mass of the devil-stick corresponding to these results is shown in Fig.3(b).

VII. CONCLUSION

The problem of juggling a devil-stick alternately between two angular configurations was addressed using DVHCs. This paper extends the work in [11], which considered *rotations* of the passive coordinate to realize propeller motion, to *oscillations* of the passive coordinate to realize planar juggling. The DVHC approach results in a rich set of juggling motions with states that are not necessarily symmetric about the vertical axis; the results for planar symmetric juggling in [8] are shown to be a special case. It is demonstrated that DVHCs are an effective tool for design and control of the trajectory of an object juggled using impacts. Similar to the zero dynamics induced by VHCs, the DZD can be used to infer the nonlinear stability characteristics of the hybrid

system subject to DVHCs, without relying on linearization about the fixed point of a Poincaré map [9]. Future work will focus on exploring a larger class of DVHCs for juggling systems and extension to other underactuated systems with impulsive inputs.

REFERENCES

- [1] A. Zavala-Rio and B. Brogliato, "On the Control of a One Degree-of-Freedom Juggling Robot," *Dynamics and Control*, vol. 9, no. 1, pp. 67–90, Jan. 1999.
- [2] B. Brogliato and A. Rio, "On the control of complementary-slackness juggling mechanical systems," *IEEE Transactions on Automatic Control*, vol. 45, no. 2, pp. 235–246, Feb. 2000.
- [3] M. W. Spong, "Impact controllability of an air hockey puck," *Systems & Control Letters*, vol. 42, no. 5, pp. 333–345, Apr. 2001.
- [4] M. Buehler, D. Koditschek, and P. Kindlmann, "Planning and Control of Robotic Juggling and Catching Tasks," *The International Journal of Robotics Research*, vol. 13, no. 2, pp. 101–118, Apr. 1994.
- [5] R. Sepulchre and M. Gerard, "Stabilization of periodic orbits in a wedge billiard," in *42nd IEEE International Conference on Decision and Control (IEEE Cat. No.03CH37475)*, vol. 2. Maui, Hawaii, USA: IEEE, 2003, pp. 1568–1573.
- [6] R. G. Sanfelice, A. R. Teel, and R. Sepulchre, "A hybrid systems approach to trajectory tracking control for juggling systems," in *2007 46th IEEE Conference on Decision and Control*, Dec. 2007, pp. 5282–5287.
- [7] S. Schaal and C. Atkeson, "Open loop stable control strategies for robot juggling," in *[1993] Proceedings IEEE International Conference on Robotics and Automation*. Atlanta, GA, USA: IEEE Comput. Soc. Press, 1993, pp. 913–918.
- [8] N. Kant and R. Mukherjee, "Non-prehensile manipulation of a devil-stick: Planar symmetric juggling using impulsive forces," *Nonlinear Dynamics*, vol. 103, no. 3, pp. 2409–2420, Feb. 2021.
- [9] —, "Juggling a Devil-Stick: Hybrid Orbit Stabilization Using the Impulse Controlled Poincaré Map," *IEEE Control Systems Letters*, vol. 6, pp. 1304–1309, 2022.
- [10] A. Khandelwal, N. Kant, and R. Mukherjee, "Nonprehensile manipulation of a stick using impulsive forces," *Nonlinear Dynamics*, vol. 111, no. 1, pp. 113–127, Jan. 2023.
- [11] A. Khandelwal and R. Mukherjee, "Discrete VHCs for Propeller Motion of a Devil-Stick using purely Impulsive Inputs," Aug. 2025. [Online]. Available: <https://arxiv.org/abs/2508.15040>
- [12] M. Maggiore and L. Consolini, "Virtual Holonomic Constraints for Euler-Lagrange Systems," *IEEE Transactions on Automatic Control*, vol. 58, no. 4, pp. 1001–1008, Apr. 2013.
- [13] A. Mohammadi, M. Maggiore, and L. Consolini, "Dynamic virtual holonomic constraints for stabilization of closed orbits in underactuated mechanical systems," *Automatica*, vol. 94, pp. 112–124, Aug. 2018.
- [14] A. Shiriaev, J. Perram, and C. Canudas-de-Wit, "Constructive tool for orbital stabilization of underactuated nonlinear systems: Virtual constraints approach," *IEEE Transactions on Automatic Control*, vol. 50, no. 8, pp. 1164–1176, Aug. 2005.
- [15] J. Grizzle, G. Abba, and F. Plestan, "Asymptotically stable walking for biped robots: Analysis via systems with impulse effects," *IEEE Transactions on Automatic Control*, vol. 46, no. 1, pp. 51–64, Jan. 2001.
- [16] N. Kant and R. Mukherjee, "Orbital Stabilization of Underactuated Systems using Virtual Holonomic Constraints and Impulse Controlled Poincaré Maps," *Systems & Control Letters*, vol. 146, p. 104813, Dec. 2020.